

# Submodeling in wear predictive finite element models with multipoint contacts

Cristina Curreli<sup>1,2</sup>  | Marco Viceconti<sup>1,2</sup>  | Francesca Di Puccio<sup>3</sup> 

<sup>1</sup>Department of Industrial Engineering, Alma Mater Studiorum – University of Bologna, Bologna, Italy

<sup>2</sup>Medical Technology Lab, IRCCS Istituto Ortopedico Rizzoli, Bologna, Italy

<sup>3</sup>Dipartimento di Ingegneria Civile e Industriale, Università di Pisa, Pisa, Italy

## Correspondence

Cristina Curreli, Department of Industrial Engineering, Alma Mater Studiorum – University of Bologna, Bologna, Italy.  
Email: cristina.curreli@unibo.it

## Abstract

The application of the submodeling technique to finite element (FE) wear analyses has been recently proposed as an efficient solution to reduce the computational cost of the simulations and provide accurate numerical results. However, the method was validated only on single point contact cases. The present study proposes a generalization of the wear submodeling procedure that can be used to speed up FE wear simulations with multipoint contacts. The modified global–local procedure is applied and evaluated on a double contact pin on plate wear test using three-dimensional models developed in Ansys® mechanical APDL. Three different model geometries with different curvature radii at the contact regions were considered in order to replicate possible critical scenarios. Results suggest that an additional wear simulation step where the global model is used to simulate the first wear cycles is needed to correctly transfer the boundary conditions to the local models. The new proposed strategy demonstrates the possibility to extend the method to more general FE wear simulations by significantly reducing their computational cost.

## KEYWORDS

finite element analysis, multipoint contact, submodeling, wear prediction

## 1 | INTRODUCTION

Finite element (FE) analysis is today one of the most powerful and robust tools used to study and predict the wear behavior of different mechanical systems. Despite the increasing performance of computers, the huge amount of computational time needed to obtain accurate wear predictions still remains the main limitation of a wider use of FE-based wear predictions. This issue is particularly important for complex three-dimensional models and is mainly due to the iterative process that is required to compute both the evolving contact pressure distribution and the incremental wear depth or volume.

Different methods were proposed in the literature in order to reduce the computational cost associated with nonlinear FE wear simulations, particularly when many loading cycles are considered. One of the most commonly used approaches is based on the so-called extrapolation technique<sup>1,2</sup> in which an extrapolation factor is selected to reduce the total number of analysis needed to estimate the final wear amount. The idea behind this method is that one FE analysis is able to represent a number of wear cycles by assuming a steady progression of wear.<sup>3</sup> A critical point of the approach is the definition of the optimum extrapolation factor. The accuracy and stability of the simulation may be thus lost by using extrapolation

This is an open access article under the terms of the Creative Commons Attribution-NonCommercial-NoDerivs License, which permits use and distribution in any medium, provided the original work is properly cited, the use is non-commercial and no modifications or adaptations are made.

© 2021 The Authors. *International Journal for Numerical Methods in Engineering* published by John Wiley & Sons Ltd.

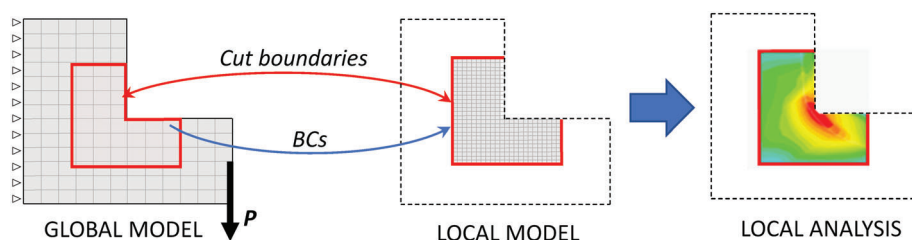


**FIGURE 1** Submodeling technique: A global model with a coarse mesh is used to estimate the boundary conditions (BCs) to be applied to the local model (LM) along the cut boundaries. Since the LM has a finer mesh compared to the global one, the accuracy of results is improved

sizes that are too large. A similar procedure was adopted by McColl et al.<sup>4</sup> that also discussed important aspects, such as mesh refinement and optimization of numbers of wear cycles for minimization of the total simulation time. Põdra and Andersson<sup>5</sup> proposed a simulation time step optimization routine able to evaluate the required integration step duration on the basis of a predefined maximum allowable wear increment. Another strategy to minimize the wear simulation time was similarly proposed by Mona et al.<sup>6</sup> that was mainly focused on the definition of the optimum time step for the geometry updates.

However, also estimating wear within a single cycle can be time consuming, especially in non-conformal contacts, where fine meshes are required. Only recently, some of the co-authors of this article proposed the application of the submodeling technique to wear problems for a single point contact (SPC).<sup>7</sup> The main idea behind the submodeling approach is that by using a combination of a global coarse model of the whole system and a local fine one of the region of interest, it is possible to reduce the computational cost and provide accurate numerical results (Figure 1).

The wear submodeling procedure mainly consists of three steps. First, a coarse FE global model (GM) is developed to provide the boundary conditions (BCs) to a refined local model (LM), which includes only a region of interest limited by the cut boundaries (CBs). Once a convergence check on the quantities to be transferred is performed, the second step regards the development of the LM with a properly defined mesh. Finally, the selected BCs are applied along the CBs and the LM is used to solve the entire wear problem.

The proposed method was validated using two-dimensional and three-dimensional models<sup>7,8</sup> with a simple pin-on-disc test configuration. Critical aspects such as the choice of the most suitable BCs and cutting regions, the role of convergence analysis in both the GM and LM and the influence of the mesh size in the contact region on the accuracy of the wear estimations were extensively discussed.

Although the wear submodeling procedure proved to be an efficient solution to the high computational cost problem, as also confirmed by Shankar et al.,<sup>9,10</sup> the main limitation of the previous study was that the discussion was restricted to a SPC case. The extension of the technique to a more general three-dimensional and multipoint contact (MPC) case is obviously of great importance. First because it concerns many applications, such as gears, rough surfaces, and knee implants. Second, the need of reducing the computational cost of FE wear simulations is particularly important when the number of the worn surfaces increases.

The present study aims at discussing this important topic and at presenting the possibility to extend the proposed wear submodeling technique to a more complex MPC case. A modified global–local procedure for FE wear models was proposed and evaluated on a double contact pin on plate wear test using three-dimensional models developed in ANSYS® MAPDL 19.3. To account for the effect of the different contact surface geometries, three-dimensional models with different curvatures were developed.

## 2 | MATERIALS AND METHODS

### 2.1 | Case study

The simple pin-on-disc wear test simulated in the previous works presented by the authors<sup>5,7</sup> was modified in a pin-on-plate test in this study in order to have equal velocity in the contact points. Moreover, to extend the wear submodeling procedure to a double contact problem, the head of the pin was modified considering an unusual profile, shown in Figure 2. Three different ratios of the curvature radii ( $\rho = r_2/r_1$ ) were assumed for achieving different contact conditions

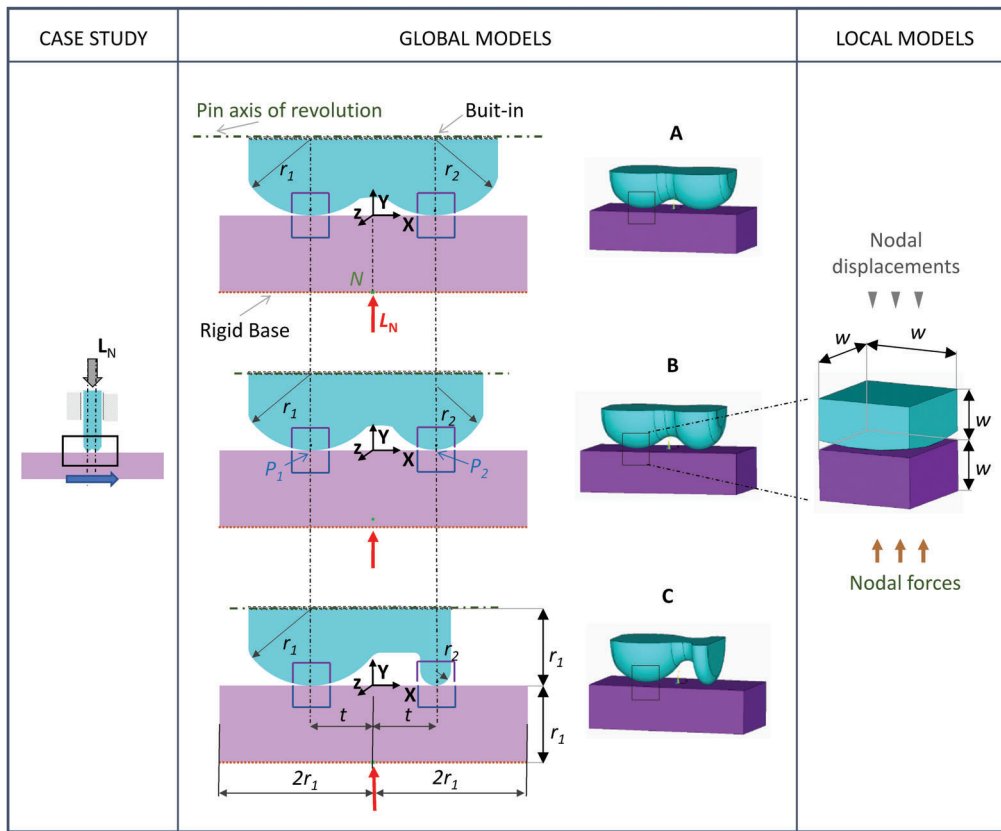


**FIGURE 2** Case study of a modified pin-on-plate wear test. BCs and geometry of the three configurations used for the submodeling procedure based on the GM and the LMs

in the two contact points ( $P_1$  and  $P_2$ ) and evaluate the effect of the different contact surfaces geometries on the wear behavior of the pin. The ratio  $\rho$  was set equal to 1, 0.6, and 0.2 for configuration A, B, and C, respectively, considering a fixed radius  $r_1 = 5$  mm (Figure 2). A constant normal load  $L_N = 42$  N was assumed for all cases.

Both the pin and the plate were virtually made of steel with elastic moduli  $E = 210$  GPa and Poisson ratio  $\nu = 0.3$ . The contact was simplified as friction free (see Section 2.3) and the material loss was attributed only to the pin, assuming that the hardness of its surface ( $H_v = 3$  GPa) was much lower than the one of the plate's surface. The wear behavior was modeled through the Archard wear law, which states that the present case the total wear volume is proportional to the normal load  $L_N$  and to the sliding distance  $d$

$$V = \frac{K}{H} L_N d, \quad (1)$$

where the dimensionless wear coefficient  $K$  was set equal to  $3.75 \times 10^{-4}$ , for this metal on metal couple. According to the Archard's theory, the total wear volume should be the same in the three cases, since it does not depend on the number or shape of the contact regions. Since wear was simulated for a total traveled distance  $d_t = 1.5$  m, the estimated total wear volume at the end of the test is  $V = 7.875 \times 10^{-3}$  mm<sup>3</sup>. However, the wear volume in each contact region cannot be easily predicted and requires numerical simulations.

## 2.2 | GM and LM: Geometry and mesh

The geometry of the three GMs and LMs used for the simulations is depicted in Figure 2. Two subregions that include the regions of interest were defined in both bodies (the plate and the pin) of the GMs with CBs at distance  $w$  far from the ideal contact points  $P_1$  and  $P_2$ . A value of the edge length  $w = 0.9$  mm was chosen so that the boundaries of the LMs could be assumed to be far enough away from the stress concentration regions.<sup>7,8</sup> The BCs for the GMs are shown in Figure 2. The top of the pin was built-in while the load  $L_N$  was applied in a pilot node  $N$ , normal to the bottom surface of the plate. Using the multipoint constraint approach, the bottom surface of the plate was constrained to a rigid translation along the  $Y$  axis.

The most convenient BCs transferred from the GMs to the LMs are given by a combination of displacements on the CBs of the wearable body (pin) and nodal forces on the CBs of the unworn body (plate) (Figure 2) as also reported in Reference 7.

Lower order 4-node tetrahedral SOLID 285 elements were chosen for the 3D mesh and CONTA173 and TARGE170 elements were used in the contact pairs for both GMs and LMs. The mesh density changes throughout the bodies, increasing in the region adjacent the contact. A convergence study, aimed at reducing the so-called “boundary error,”<sup>11</sup> defined a minimum element edge size  $h_G = 45 \mu\text{m}$  ( $w/20$ ) at the contact surfaces of the GMs while a mesh outside the CBs was kept fixed with a maximum element edge size of 0.5 mm ( $r_1/10$ ) far from the contact regions. In Reference 7, where the GM was used only for defining the BCs of the LM, the mesh in the contact region was coarser. In the present case, a fine mesh is defined since the GM is used also for wear simulations.

In the LMs, a minimum element size of  $h_L = 45 \mu\text{m}$  ( $w/20$ ) was set at the contact surfaces. In the previous work,<sup>7</sup> interesting results on the influence of the mesh size on the accuracy of wear estimation suggested that an element size of about  $h_L = w/20$  was also enough to accurately predict the total wear volume: a relative error ( $e_A$  (%)) between the numerical and the theoretical wear volume that reached 10% at the beginning of the wear process, was reduced to 1% after a sliding distance of about 600 mm. An element size of  $90 \mu\text{m}$  ( $w/10$ ) was defined along the CBs in both GMs and LMs.

The LESIZE and the NREFINE commands were used to generate a smooth mesh transition and to progressively refine the mesh in the contact regions.

### 2.3 | Contact model and wear implementation

The first step in wear modeling is a contact analysis. Indeed, contact pressure and sliding distance are two typical inputs of the wear law, for example, Archard law. As far as contact pressure is concerned, when friction is rather low (i.e., coefficient of friction lower than 0.10), it is usually assumed that it is only slightly affected by friction.<sup>12</sup> Thus, a friction free contact is considered in the models. However, it is worth noting that this hypothesis does not imply that there is no wear, since wear evaluation is independent from the frictionless/frictional contact behavior in FE codes.

The default augmented Lagrangian algorithm with an automatic stiffness calculation for both GM and LM was assumed. The contact detection was located at nodal points using the surface projection based contact method.

For wear calculation, the TB,WEAR routine with the Archard law option was used to automatically compute the progressive loss of material and update the geometry. The rate of wear depth is calculated by the following equation:

$$\frac{\Delta h}{\Delta t} = \frac{K}{H} p^m v^n, \quad (2)$$

where  $H$  is the material hardness,  $K$  is the dimensionless wear coefficient, and  $m$  and  $n$  are, respectively, the pressure and velocity exponent, variable with the wear law. In order to reduce the computational time, the sliding of the pin on the plate was not explicitly modeled and a fictitious wear coefficient  $K_v = 9.375 \times 10^{-3}$  mm/s that includes the constant speed at the contact nodes was specified in the TB,WEAR command for all the contact pairs.

The wear depth increment is calculated at each iteration and assigned to the contact elements of the wearing surfaces, as nodal displacement producing the estimated progressive loss of material.

The NLADAPTIVE command was used to automatically smooth the distorted elements during the wear simulation. A mesh nonlinear adaptivity (NLAD) criterion equal to 0.8 was chosen for the remeshing process: when the ratio between the wear volume and the initial volume of the solid elements underlying the contact ones exceeds 0.8, the program restarts the analysis with an improved mesh.

An automatic time stepping was used for the analyses by setting, with DELTIM command, the minimum and the maximum time step size of 0.001 and 0.1, respectively. The entire wear simulations were computed with an Intel Core i7-9700 at 3 GHz and 64 GB RAM. A distributed memory parallel scheme was adopted with two processors.

### 2.4 | Issue of an MPC problem and new procedure definition

When dealing with generic MPC problems, it is necessary to consider some potential issues related to the application of the original wear submodeling procedure proposed in the previous study for a SPC case.<sup>7</sup> The reason can be explained by considering the simple schematic example depicted in Figure 3. For an SPC problem, the constant load  $L_N$  applied

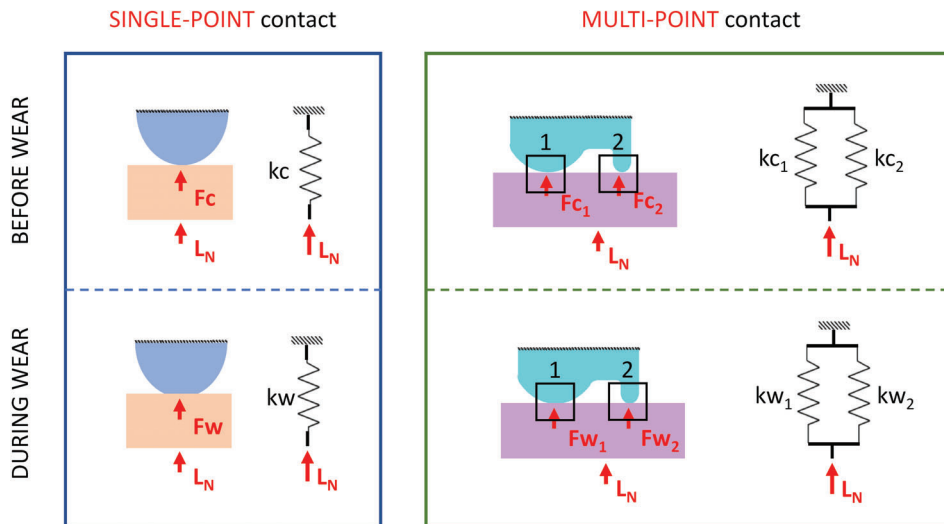


**FIGURE 3** Schematic example that helps to describe the differences in terms of total contact force distribution on the contact surfaces before and during wear for a single point (left) and multipoint contact and wear problem (right)

at the bottom surface of the plate is entirely transferred to the contact surfaces and its value does not vary during wear ( $L_N = F_c = F_w$ ). The BCs can be extracted from the GM contact analysis and kept constant for the whole wear simulation performed with the LM as long as the CBs are set far enough from the region of stress concentration.<sup>7</sup> On the contrary, for an MPC case,  $L_N$  is generally split in two or more contact forces (here  $F_{c1}$  and  $F_{c2}$ ) whose values depend on the stiffness of the parts ( $k_{c1}$  and  $k_{c2}$ ). The forces  $F_{c1}$  and  $F_{c2}$  may vary during the wear process, in particular if the ratio of the contact stiffness varies during wear. This can happen, for example, as a result of different contact geometries and different wear rates ( $k_{c1}/k_{w1} \neq k_{c2}/k_{w2} \Rightarrow F_{c1} \neq F_{w1}$  and  $F_{c2} \neq F_{w2}$ ). It must be added that, in non-conformal contacts, the stiffness is typically load-dependent, thus it is not easy to predict how contact forces vary with wear. However, the rate of force and stiffness variation is expected to be high in the first running-in phase, when surfaces in contact progressively adapt to each other, while it decreases markedly in the quasi-steady state condition. In general, it can be assessed that when transferring the BCs to the LMs, it is important to verify not only that the CBs are at a “safe distance” from the region of stress concentration and that the “boundary error” is acceptable but also that the running-in phase is completed so that the total contact force acting on the contact surfaces included in the regions of interest is almost constant.

A modified version of the wear submodeling procedure presented in the previous study is thus proposed in this work. The general flow-chart is depicted in Figure 4. With respect to the workflow proposed for the SPC problem,<sup>7</sup> an additional wear simulation step is introduced in the GM analysis. The FE global model is used to solve the contact problem and to simulate the first wear cycles (i.e., running-in phase). Once a specific transfer criterion that identifies the end of the running-in phase is met (described in Section 2.5), the wear analysis performed with the GM is stopped and the BCs are transferred to the LMs, used to simulate the rest of the entire wear test (Figure 4). It is worth noting that the LMs are now developed using the updated geometry within the regions of interest extracted from the final unloaded configuration of the GM wear analysis. The UPGEOM command in ANSYS® MAPDL was used to get the deformed mesh of the worn body.

## 2.5 | GM to LM transfer criterion

A fundamental point for the application of the proposed procedure is thus the identification of the end of the running-in phase for moving from a GM to a LM simulation. In non-conformal contacts, as in the present case, a rapid adaptation of the contact surfaces is expected, with a growth of the contact areas. As a result, the value of the maximum contact pressure, which is usually very high in the initial cycles, rapidly decreases as wear evolves. A qualitative trend of the  $p_{\max}$  with the sliding distance  $d$  during the first wear phase is shown in Figure 5. The end of the running-in phase can be identified by considering the value of  $d$  at which the curve that approximates the evolution of  $p_{\max}$  starts to “flatten.”

A transfer criterion was thus introduced by looking at the dimensionless quantity TSR defined as the ratio between the incremental (CPR) and the average (APR) contact pressure rate:

$$\text{TSR}^i = \frac{\text{CPR}^i}{\text{APR}^i} = \frac{(p_{\max}^{i+1} - p_{\max}^i)/(d^{i+1} - d^i)}{(p_{\max}^i - p_{\max}^0)/d^i}, \quad (3)$$



**FIGURE 4** FE wear submodeling procedure for multipoint contact and wear problems consisting of four main steps: (1) development of the GM, (2) wear simulation using the GM, (3) development of the LM, and (4) wear simulation using the LMs

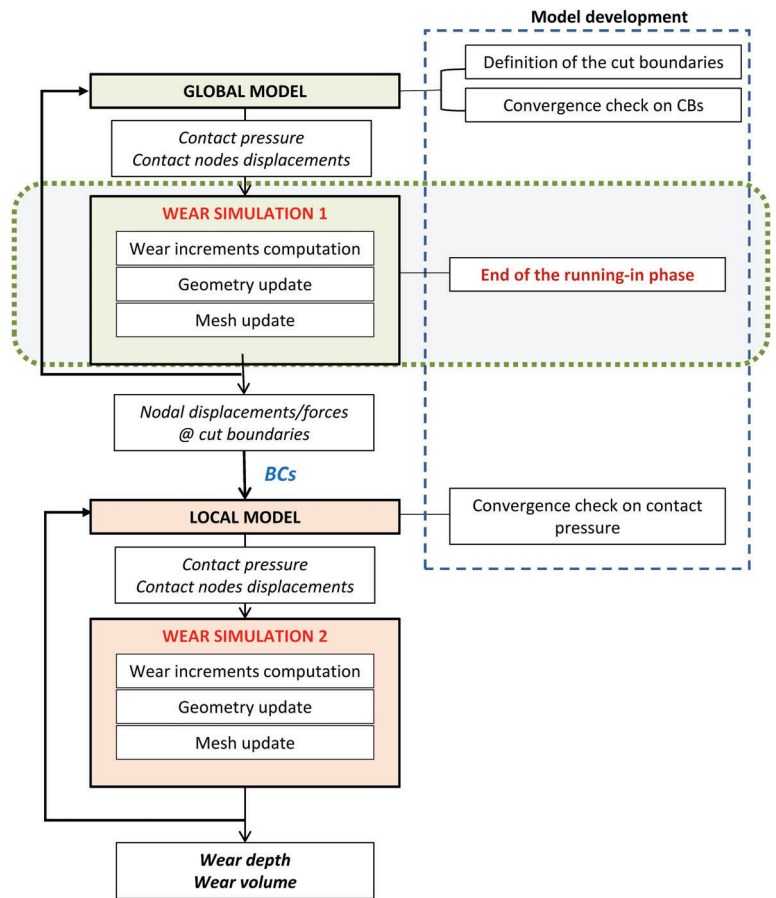
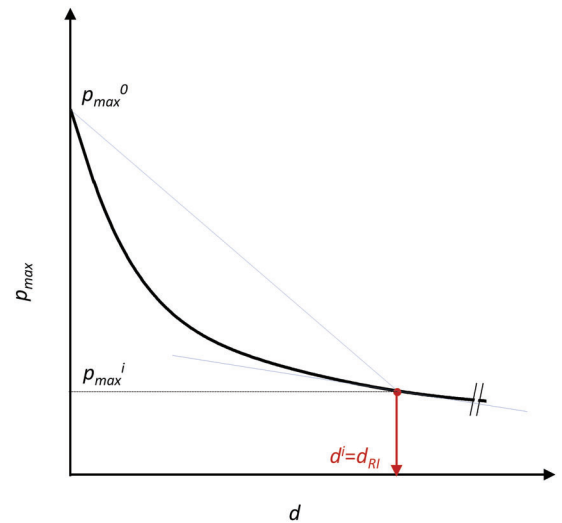


**FIGURE 5** Generic trend of the  $p_{max}$  during the first wear phase and definition of the criterion adopted to identify the end of the running-in phase



where superscript  $i$  refers to the substep number at which the wear solution results obtained with the GM are analyzed and  $p_{max}^0$  is the value of the maximum contact pressure in the unworn condition. In this study, the running-in phase is assumed to end when  $TSR < 0.15$ . The value of  $d$  that corresponds to this value of the TSR is called hereinafter  $d_{RI}$ . Since “irregularities” in the numerical derivative (CPR) can occur, it is recommended to check the application of this criterion with the visual observation of the global trend of  $p_{max}$ .

## 2.6 | Evaluation scheme

In order to evaluate the validity of the proposed method, the results obtained adopting the new FE wear submodeling procedure were compared with the ones obtained simulating the same wear test with the GM. Since the objective of this

work was to develop a more efficient approach to the problem at hand, a third modeling method is also considered when comparing the results in terms of accuracy in predicting wear versus computational cost (expressed as CPU-time, e.g., core-hours). As already mentioned in Section 2.4, the LMs are developed using the updated geometry extracted from the final unloaded configuration of the GM wear analysis. However, the procedure can be further simplified avoiding the transfer of the geometry/mesh from the GM to the LMs at the end of the running-in phase, a step that might require the use of reverse engineering tools.

The three modeling methods considered in the comparative analysis, which will be presented and discussed in Section 3.3, are the following.

- i. *No submodeling*: The GM is used to simulate the entire wear test. The wear volume, contact area, and maximum contact pressure predicted by this model are the reference values against which the accuracy of the others is compared.
- ii. *Full MPC wear submodeling*: The GM is used to simulate wear until the traveled distance reaches the running-in limit ( $d = d_{RI}$ ). The BCs are then extracted, together with the deformed mesh/geometry, and transferred to LMs used to simulate the rest of the test.
- iii. *Partial MPC wear submodeling*: The GM is used to simulate wear until the traveled distance reaches the running-in limit. The BCs are then extracted and transferred to the LMs that are used to simulate the whole wear test.

For each of the two submodeling methods, the computational cost to compute the solution for a single and for both regions of interest is provided.

### 3 | RESULTS AND DISCUSSION

#### 3.1 | Wear analyses on the GMs (no submodeling)

In order to define a reference solution for the MPC submodeling procedure, as first step, wear predictions were obtained for the three cases (A, B, and C) by means the GMs. To ensure the same level of accuracy, the mesh of the GMs in the subregions was defined as in the LMs.

The trends of the contact forces  $F_1$  and  $F_2$  in the two contact regions are shown in Figure 6 for the three geometries. As expected, the two forces are almost equal for case A during the whole test. On the other side, for cases B and C,  $F_1 > F_2$  (since the higher the contact radius the higher stiffness) with a difference that increases with  $d$  (and wear), keeping always  $F_1 + F_2 = L_N = 42$  N. The running-in phase, when forces change rather rapidly, appears to be completed for  $d = 50$  mm (as shown in the plot detail) although a kind of oscillatory trend remains in the solution, due to numerical issues and mesh size.

The plots of the wear volumes are reported in Figure 7(A), for each contact region and as total wear volume of the pin. It can be observed that the total wear volume for the three cases (A, B, and C) is the same and is linear with  $d$ , as

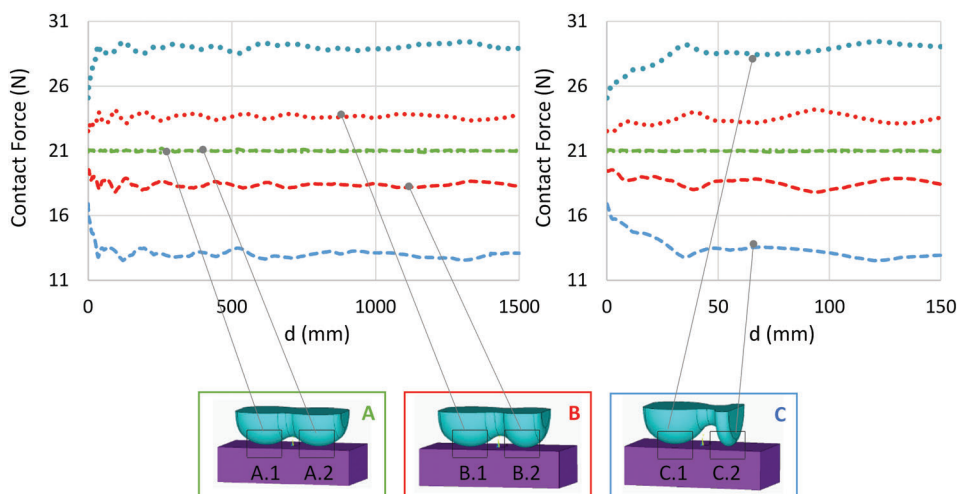
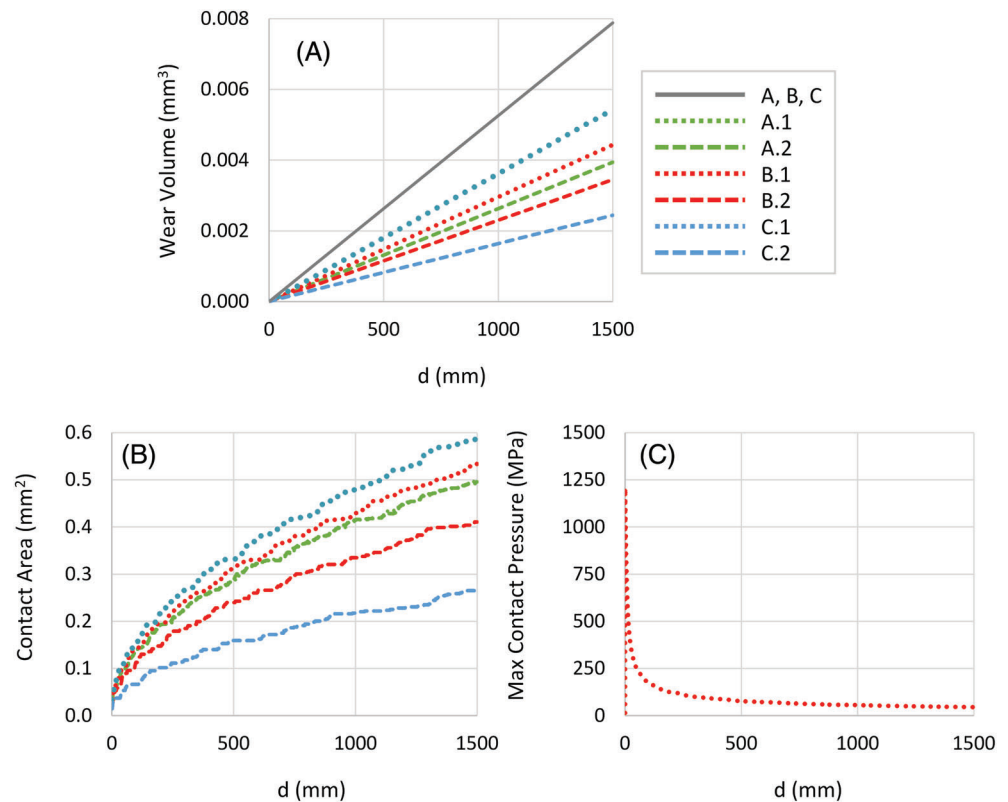


**FIGURE 6** Contact forces in the two contact points during wear for the three geometries: A, B, C. Left: Complete wear test, right: detail of the initial phase

**FIGURE 7** Total and local wear volumes of the pin for of the three geometries A, B, C (A). Evolution of the contact areas (B) and of the maximum contact pressure (C) during the wear test



predicted by Equation (1). This confirms the correct implementation of the Archard wear law for the problem (percentage error on the total wear volume less than 0.1%). According to Figure 7(A), also the local wear volumes in the two contact regions increase linearly, despite the contact forces are not constant for cases B and C. This means that the variation of the contact force, marked in the first part of the test, affects only marginally the wear results. Figure 7(B,C) presents the results in term of contact areas and contact pressure evolution during the wear test. The contact areas show very marked increments, reaching about 17 times their initial value. As for the contact forces, the trends of the areas with wear are not smooth, they both are related to the mesh. On the other side, the behavior of the maximum contact pressure  $p_{\max}$  appears more regular (Figure 7(C)), with a rapid decrease in the running-in phase. In Figure 7(C), only the trend of  $p_{\max}$  in B.1 is plotted since the curves for the other contact points would be all almost overlapped to it. It can be noticed that, at the end of the wear test,  $p_{\max}$  is about 45 MPa, 3.7% of its value in the unworn condition.

Another interesting result regards the difference in the contact pressure values in the two contact regions, which decreases during the wear process for all three cases. For example, in case C, where the initial curvatures in the ideal contact points were very different, the initial maximum pressures differed of about 600 MPa, while at  $d = 50$  mm the difference was already as low as 20 MPa. At the end of the wear test almost no differences could be noticed in the value of  $p_{\max}$  in the two contact regions. Thus, wear appears as a kind of “democratic” process that fosters a uniform distribution of the contact pressure.

### 3.2 | End of the running-in phase

As already stressed, the application of the proposed submodeling procedure to MPC is based on a fundamental step: the identification of the end of the running-in phase for moving from a GM to the LMs. Figure 8(A,B) shows the trend of  $P_{\max}$  and of the quantity TSI (Section 2.5) during the first wear phase in one of the two contact regions for cases A, B, and C. It can be noticed that the transfer criterion is met when  $d = d_R = 50$  mm. The value TSR is less than 0.15 for all the three cases after simulating wear for about 1/30 of the entire test.

As also happens in this example, a noisy behavior of the quantity TSR reported in Figure 8(B) can be observed. In order to avoid this problem and to precisely identify  $d_{RI}$ , some fitting or filtering post processing operations can be done.



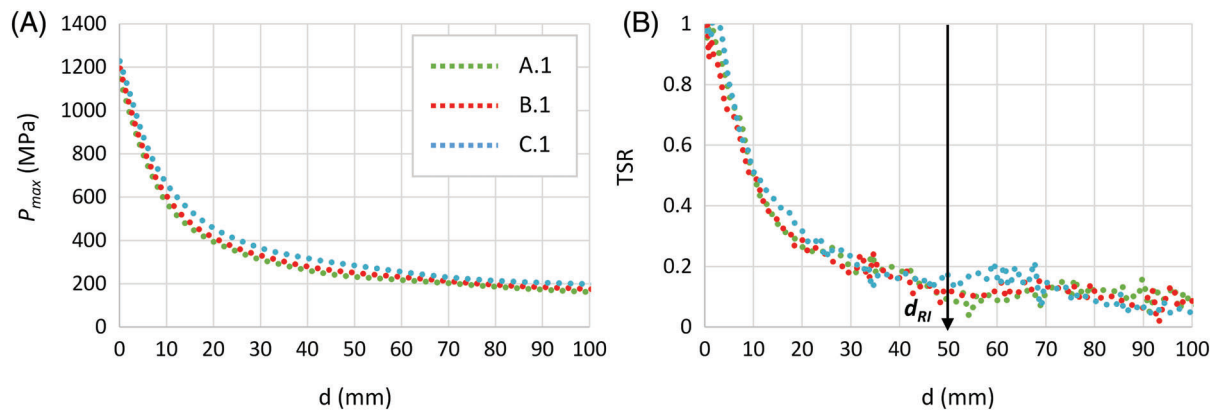


**FIGURE 8** Trend of  $P_{\max}$  (A) and of TSR (B) with increasing values of  $d$  during the initial wear phase and identification of  $d_{RI}$

However, it is worth stressing that capturing the exact threshold value is not so important. In general, a higher threshold implies longer computational time while a lower one could introduce small error in results. The criterion to identify the end of the running-in phase used in this study ( $TSR < 0.15$ ) can be considered a general suggestion that can be reasonably applied to other cases as well. It is also important to notice that the identification of the value of  $d_{RI}$  plays a fundamental role in deciding whether to apply the wear submodeling procedure or not. For example, passing from GM to LMs could be useful if the total traveled distance  $d_t$  is 10 times higher than the distance of the running-in phase ( $d_{RI}$ ), which for the present problem would mean  $d_t > 500$  mm. Indeed, it must be considered that a certain effort is required to transfer data from the GM to the LM and before doing it, it can be worth doing a balance between residual distance of the wear test and efforts to change model.

### 3.3 | Wear results with LMs and procedure validation

In order to validate the MPC wear submodeling procedure, the wear results related to contact regions A.1, B.1, and C.1, presented for the GMs in Section 3.1, were compared with the ones obtained simulating the same wear test with the GMs up to  $d_{RI}$  and with the LMs after it, adopting the TSR criterion for model transfer (Section 2.5). As mentioned in Section 2.6, also a third modeling method, where the procedure is further simplified avoiding the transfer of the geometry/mesh from the GM to the LM at the end of the running-in phase, is considered in the comparative analysis. The results obtained with the so called *no submodeling*, *full MPC wear submodeling*, and *partial MPC wear submodeling* methods in terms of maximum contact pressure, wear volumes and contact areas at the end of the simulated wear test are reported in Table 1. It can be observed that, for all the three different simulated cases, the results obtained using the three approaches are very similar with discrepancies always lower than 1.5%. As expected, for case A, the results are almost identical (percentage differences lower than 0.12%, 0.08%, and 0.001%, respectively, for contact pressure, wear volume, and contact areas). Slightly higher discrepancies can be noticed for cases B and C (maximum difference is about 1.47% for case C on the total wear volume); this might be explained by considering the oscillatory trend of the contact force during the running-in phase (Figure 6).

It is important to underline that, in this work, the mesh density of the GMs has been selected based on a convergence analysis which aims at reducing the “boundary error” or “interface error.” However, because the GMs are now used to solve not only the contact problem but also to simulate the first wear cycles, a mesh convergence check on the maximum contact pressure might be added if a high level of wear predictive accuracy is needed in the first phase. Preliminary mesh convergence studies on case A, suggested that a finer mesh in the contact regions of the GMs will also help to reduce the oscillatory behavior of the contact force in the running-in phase (Figure 6) by increasing the level of accuracy in capturing the BCs. As also discussed in the previous work,<sup>7</sup> the choice of the most suitable contact element size when developing FE wear models is a critical aspect. The modeler must find a balance between two opposite requirements: high predictive accuracy and low computational time.

Another important aspect that is worth considering is that, while the results obtained with the two submodeling approaches (full and partial) at the end of the wear test are almost identical, significative differences can be observed in

**TABLE 1** Comparison of three procedures: wear predictions with GM and application of submodeling (full and partial) with transfer from GM to LM

		Max contact pressure (MPa)	Wear volume ( $\times 10^{-3}$ mm <sup>3</sup> )	Contact area (mm <sup>2</sup> )
No submodeling	A.1	42.492	3.941	0.499
	B.1	44.776	4.433	0.535
	C.1	49.468	5.428	0.587
Full MPC wear submodeling	A.1	42.448	3.938	0.499
	B.1	44.922	4.374	0.528
	C.1	49.190	5.348	0.585
Partial MPC wear submodeling	A.1	42.442	3.938	0.499
	B.1	44.901	4.373	0.528
	C.1	49.173	5.351	0.585

**TABLE 2** Comparison of the three modeling methods in term of accuracy versus computational cost

		Max wear volume error (%)	Computational cost single region (core-hours)	Computational cost two regions (core-hours)
No submodeling	–	–	59	–
MPC wear submodeling	A.1	0.076	21	31.5
	B.1	1.330	–	–
	C.1	1.473	–	–
Partial MPC wear submodeling	A.1	0.076	22	32
	B.1	1.353	–	–
	C.1	1.418	–	–

the first wear phase. In particular, for cases B and C, the results in term of volume loss are almost identical only after  $d = 80$  and  $d = 750$ , respectively. It can be stated that if the value of  $d_{RI}$  is small (the computational effort required to repeat the first wear cycles already simulated with the GM is not considerable) and the focus is on the final wear of the surfaces (not on every single initial step) the transfer process of the updated worn geometry could be eliminated and LM used for the whole wear test simulation using BCs obtained from the GM at the end of the running-in phase.

Undoubtedly, the most interesting results of this study regard the comparison in term of accuracy versus computational costs, as reported in Table 2. The GMs took almost 29 h and 35 min to simulate the entire wear test while, by applying the full and partial MPC wear submodeling technique, the final results, related to one of region of interest, were obtained with less than half a day (10 h, 30 min, and 11 h, respectively). The huge difference in computational time is obviously due to a significant reduction of the three-dimensional model size used for the LM simulations (the GM contains a number of nodes of about 3.5 times higher than the LM) and in particular to the fact that multiple contact and wear problems were reduced to SPC and wear problems for more than 95% of the entire test. From Table 2, it is possible to observe that the application of the wear submodeling procedure helps to significantly reduce the computational time also when wear is simulated in both regions.

## 4 | CONCLUSIONS

This article discusses the limitations of the wear submodeling procedure recently presented by the authors for a single contact point and proposes the extension of the method to more general multipoint problems. In order to confirm that the modified global–local procedure does not significantly reduce the predictive accuracy of the model, a pin-on-plate

wear test was simulated here considering a double-headed pin. Three different model configurations with different pin curvature radii were considered in order to evaluate the effect of the different contact surfaces geometries on the wear behavior of the pin.

The general behavior obtained from the simulations describes a linear trend of the total wear volume equal for all cases. However, the way the total volume is distributed in the two contact regions of each model is different for the three cases. Although looking at the wear volume the process shows a constant rate, this is not the case observing the trends of maximum pressure and contact area. In fact, as expected in non-conformal contacts, in the initial period wear occurs in a small region causing a rapid adaptation of the contact surfaces with a reduction of maximum pressure values. This is usually described as the running-in phase, that it is followed by a steady state condition. In some cases, these two phases are characterized also by different wear coefficients, higher in the running-in. The transition between the two stages is critical also for defining the correct simulation procedure. Indeed, when dealing with MPC and wear problems, the BCs can be extracted from the GM wear simulations and transferred to LM wear analyses once the running-in phase is completed. Thus, the GM is used not only for the contact analyses but also to simulate the first wear cycles. A hybrid submodeling technique, where forces and displacements were extracted directly from the GMs and then combined to provide the BCs for the local ones, proved to be an efficient and suitable solution also for MPC problems. As further simplification, another procedure has been also proposed: depending on the extension of the simulated wear time with respect to the initial running-in phase and on the aim of the analysis, it can be convenient to adopt the LMs for the whole process, with BCs corresponding to the end of the running-in.

The present study demonstrates the possibility to successfully extend the wear submodeling technique to MPC cases and significantly reduce the computational cost of generic FE wear analyses. The method seems to be particularly useful to speed up FE wear simulations where a high level of accuracy is needed only in a specific contact region or when many different wear analyses need to be performed, for example, in case of design sensitivities analyses.


## DATA AVAILABILITY STATEMENT

The data that support the findings of this study are available from the corresponding author upon reasonable request.

## ORCID

Cristina Curreli  <https://orcid.org/0000-0002-9904-3849>

Marco Viceconti  <https://orcid.org/0000-0002-2293-1530>

Francesca Di Puccio  <https://orcid.org/0000-0003-4558-1497>

## REFERENCES

- Mukras S, Kim NH, Sawyer WG, Jackson DB, Bergquist LW. Numerical integration schemes and parallel computation for wear prediction using finite element method. *Wear*. 2009;266:822-831. <https://doi.org/10.1016/j.wear.2008.12.016>.
- Kim NH, Won D, Burris D, et al. Finite element analysis and experiments of metal/metal wear in oscillatory contacts. *Wear*. 2005;258:1787-1793. <https://doi.org/10.1016/j.wear.2004.12.014>.
- Mattei L, Di Puccio F. Influence of the wear partition factor on wear evolution modelling of sliding surfaces. *Int J Mech Sci*. 2015;99:72-88. <https://doi.org/10.1016/j.ijmecsci.2015.03.022>.
- McColl IR, Ding J, Leen SB. Finite element simulation and experimental validation of fretting wear. *Wear*. 2004;256:1114-1127. <https://doi.org/10.1016/j.wear.2003.07.001>.
- Pödra P, Andersson S. Simulating sliding wear with finite element method. *Tribol Int*. 1999;32:71-81. [https://doi.org/10.1016/S0301-679X\(99\)00012-2](https://doi.org/10.1016/S0301-679X(99)00012-2).
- Öqvist M. Numerical simulations of mild wear using updated geometry with different step size approaches. *Wear*. 2001;249:6-11. [https://doi.org/10.1016/S0043-1648\(00\)00548-2](https://doi.org/10.1016/S0043-1648(00)00548-2).
- Curreli C, Di Puccio F, Mattei L. Application of the finite element submodeling technique in a single point contact and wear problem. *Int J Numer Methods Eng*. 2018;116:708-722. <https://doi.org/10.1002/nme.5940>.
- Curreli C, Mattei L, Di Puccio F. Finite element simulations of pin-on-disc wear tests using submodeling. Paper presented at: AIMETA 2017, Salerno—Proceedings of the 23rd Conference of the Italian Association of Theoretical and Applied Mechanics. Vol 4; 2017:587-593.
- Shankar S, Nithyaprakash R, Santhosh BR, Uddin MS, Pramanik A. Finite element submodeling technique to analyze the contact pressure and wear of hard bearing couples in hip prosthesis. *Comput Methods Biomech Biomed Eng*. 2020;23:422-431. <https://doi.org/10.1080/10255842.2020.1734794>.
- Shankar S, Nithyaprakash R, Santhosh BR, Gur AK, Pramanik A. Experimental and submodeling technique to investigate the wear of silicon nitride against Ti6Al4V alloy with bio-lubricants for various gait activities. *Tribol Int*. 2020;151:106529. <https://doi.org/10.1016/j.triboint.2020.106529>.

11. Cormier NG, Smallwood BS, Sinclair GB, Meda G. Aggressive submodelling of stress concentrations. *Int J Numer Methods Eng*. 1999;46:889-909. [https://doi.org/10.1002/\(SICI\)1097-0207\(19991030\)46:6<889::AID-NME699>3.0.CO;2-F](https://doi.org/10.1002/(SICI)1097-0207(19991030)46:6<889::AID-NME699>3.0.CO;2-F).
12. Mattei L, Di Puccio F. Wear simulation of metal-on-metal hip replacements with frictional contact. *J Tribol*. 2013;135:1-11. <https://doi.org/10.1115/1.4023207>.

**How to cite this article:** Curreli C, Viceconti M, Di Puccio F. Submodeling in wear predictive finite element models with multipoint contacts. *Int J Numer Methods Eng*. 2021;122:3812–3823. <https://doi.org/10.1002/nme.6682>